

Optimizing GaN/AlGa_xN Multiple Quantum Well Structures by Time-Resolved Photoluminescence

J. Li, K. C. Zeng, E. J. Shin, J. Y. Lin, and H. X. Jiang^{a)}

Department of Physics, Kansas State University, Manhattan, KS 66506-2601

ABSTRACT

We present the results of picosecond time-resolved photoluminescence (PL) measurements for GaN/Al_xGa_{1-x}N MQWs with varying structural parameters, grown by metalorganic chemical vapor deposition under the optimal GaN-like growth conditions. We have shown that the optimal GaN/AlGa_xN ($x \sim 0.2$) MQW structures for UV light emitter applications are those with well widths ranging from 12 and 42 Å and barrier widths ranging from 40 to 80 Å. The decreased quantum efficiency in GaN/Al_xGa_{1-x}N MQWs with well width $L_w < 12$ Å is due to the enhanced carrier leakage to the underlying GaN epilayers, while the decreased quantum efficiency in MQWs with well width $L_w > 42$ Å is associated with an increased nonradiative recombination rate as L_w approaching the critical thickness of MQWs. For the barrier width dependence, when the barrier width is below the critical thickness, the nonradiative recombination rate increases with a decrease of the barrier width due to the enhanced probabilities of the electron and hole wavefunctions at the interfaces as well as in the AlGa_xN barriers. On the other hand, the misfit dislocation density increases as the barrier width approaches the critical thickness, which can result in an enhanced nonradiative interface recombination rate. Our optimized GaN/Al_xGa_{1-x}N MQW structures exhibited extremely high quantum efficiencies as well as a ratio of well emission intensity to barrier emission intensity exceeding 10^4 .

Keywords: GaN/AlGa_xN quantum wells, wide bandgap, time-resolved PL, optical transitions, UV light emitters

1. INTRODUCTION

The group III-nitride semiconductors consisting of AlN, GaN, InN and their alloys are recognized as very promising materials for many optoelectronic device applications such as blue-green and UV light emitting diodes (LEDs), laser diodes (LDs), UV solar blind detectors, and high-temperature/high-power electronic devices [1]. Because many III-nitride based devices have utilized the advantages of multiple-quantum-well (MQW) structures, the optical properties of GaN/Al_xGa_{1-x}N MQW structures are of great current interest[2-10]. For the optimization of LEDs and LDs structures, it is crucial to maximize the optical emission or quantum efficiencies (QE) in the quantum confined states in the well regions. It is expected that the QE of MQWs depend strongly on the growth conditions. For the growth of GaN/Al_xGa_{1-x}N MQWs, one can choose the growth conditions to be the optimal growth conditions of either GaN epilayers (GaN-like) or Al_xGa_{1-x}N epilayers (Al_xGa_{1-x}N-like). It was demonstrated that the optimal growth conditions for GaN/AlGa_xN MQWs by metal organic chemical vapor deposition (MOCVD) are GaN-like [8-10]. On the other hand, the MQW structural parameters such as the well and barrier widths are expected to affect the QE as well.

A set of 50 Å barrier GaN/Al_xGa_{1-x}N ($x \approx 0.2$) MQWs with well widths, L_w , varying from 6 to 48 Å, and another set of 30 Å well GaN/Al_xGa_{1-x}N MQW structures with varying barrier widths from 30 to 100 Å have been grown by MOCVD under the optimal GaN-like growth conditions. Picosecond time-resolved photoluminescence spectroscopy has been employed to probe the well-and barrier width dependencies of the quantum efficiencies (QE) of these MQWs. Our results have shown that these GaN/AlGa_xN MQW structures exhibit negligibly small piezoelectric effects and hence enhanced QE. It was observed that, GaN/Al_xGa_{1-x}N MQWs with L_w between 12 and 42 Å provide the highest QE, which can be attributed to the reduced nonradiative recombination rate as well as the improved quantum-well quality. The decreased QE in GaN/Al_xGa_{1-x}N MQWs with $L_w < 12$ Å is due to the enhanced carrier leakage to the underlying GaN epilayers, while the decreased QE in MQWs with $L_w > 42$ Å is associated with an increased nonradiative recombination rate as L_w approaching the critical thickness of MQWs. On the other hand, our results revealed that the QE and the recombination lifetime of these 30 Å well GaN/Al_xGa_{1-x}N MQWs increase with an increase of the barrier width up to 80 Å. These behaviors can be explained by two different effects in MQWs: (1) enhanced nonradiative recombination rates in MQWs of narrower barrier widths due to enhanced probabilities of the electron and hole wavefunctions at the interfaces as well as in the barriers (at $L_B \leq 80$ Å) and (2) enhanced nonradiative recombination rates in MQWs due to an increased misfit dislocation density at the interfaces when the barrier width approaches the critical thickness, $L_B \sim 100$ Å.

2. EXPERIMENTAL

The GaN/Al_xGa_{1-x}N ($x \approx 0.2$) MQW samples were grown on 0001-oriented sapphire substrates under the optimal GaN-like growth conditions by MOCVD [8]. The growth temperature and pressure were 1050 °C and 300 Torr, respectively. Prior to the growth of the MQWs, a 250 Å GaN buffer layer and a 1.3 μm undoped GaN epilayer were grown on the sapphire substrate. It was then followed by the growth of the MQW structure with thirty periods of GaN well and Al_xGa_{1-x}N barrier. The MQW samples were terminated by 250 Å thick Al_xGa_{1-x}N cap layers with the same composition as the barriers. The Al molar fraction in Al_xGa_{1-x}N barriers was targeted at 20%. For the set of MQWs with varying well widths, the barrier width was fixed at 50 Å and the well widths of these samples were 6, 12, 18, 24, 30, 36, 42, and 48 Å. For the a set of 30 Å well GaN/Al_xGa_{1-x}N MQWs, the barrier width was targeted to vary from 30 to 100 Å. The well and barrier widths were determined by the growth rates of the GaN and Al_xGa_{1-x}N epilayers under the optimal GaN-like growth conditions.

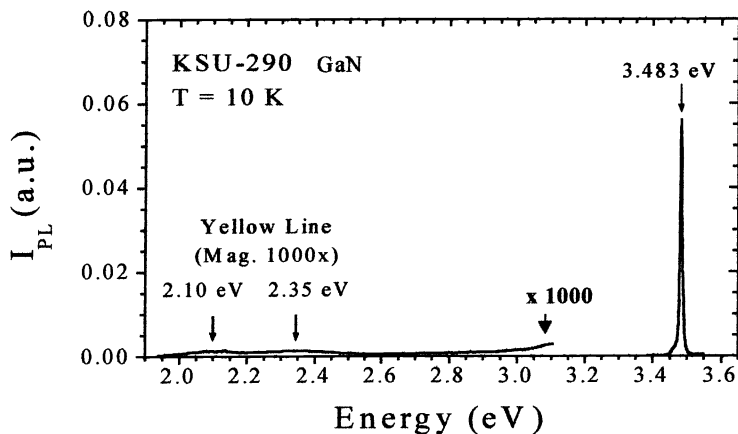


Fig. 1 Low temperature PL spectrum for one of our GaN epilayers recorded in a large emission energy scale to include yellow emission lines. The PL signal in the low energy region ($E < 3.1$ eV) has been magnified by a factor of 1000, indicating very little contribution from yellow emission and hence the high crystalline quality and purity of our samples.

The low temperature PL spectrum for one of our representative GaN epilayers grown under the same conditions as those of GaN epilayers underneath the MQWs studied here is shown in Fig. 1. One can see that our as-grown GaN epilayers on sapphire substrates emit only the exciton transitions at 3.483 eV with a full-width-at half-maximum (FWHM) of about 4 meV (the ratio of the exciton emission intensity to the yellow line intensity exceeds 10^4). The typical room temperature electron concentration and mobility of our undoped 3 μm thick GaN epilayers are about $5 \times 10^{16} \text{ cm}^{-3}$ and $650 \text{ cm}^2/\text{Vs}$, respectively. Picosecond time-resolved photoluminescence (PL) spectroscopy [11] was employed to study the optical properties of these MQWs. The excitation wavelength and average pumping power were 290 nm and 20 mW, respectively. The time-resolved PL signals were dispersed by a 1.3 m monochromator and collected either by a single-photon counting detection system or a streak camera (Hamamatsu C5680) with a time resolution of 25 ps or 2 ps.

2. RESULTS AND DISCUSSIONS

2.1 Well width dependence

The cw PL spectra of GaN/AlGa_xN MQWs with varying well widths measured at 10 K are shown in Fig. 2. The main emission peaks (varying from 3.507 to 3.693 eV) in these spectra are due to the excitonic recombinations in the GaN-well regions. The low energy emission peaks around 3.490 eV are from the underlying undoped GaN epilayers. No transition peaks from the Al_xGa_{1-x}N-barrier regions are observed, indicating that the PL emission and carrier confinement in the well regions are highly efficient, which is consistent with our previous result that barrier transition is absent in GaN/Al_xGa_{1-x}N MQWs grown under the optimal GaN-like growth conditions [8]. The PL emission spectral peak position as a function of the well width is shown in Fig. 3. Compared with the emission peaks from the underlying GaN layers around 3.490 eV, the main emission peaks from the quantum wells are all blue shifted, which results from both the quantum confinement and the biaxial compressive strain in the well regions.

From Fig. 2, the linewidths of the well emission peaks of these MQWs replotted in Fig. 4 are between 25 and 35 meV, which are among the narrowest values reported for the GaN/Al_xGa_{1-x}N MQW system. This indicates that the interface quality of these MOCVD grown MQWs is reasonably high, which should result in more efficient carrier confinement in these MQWs. An increased interface quality can also lead to a decreased nonradiative recombination rate at the interface and thus an enhanced radiative recombination rate or higher QE in the quantum wells.

The integrated well emission intensity versus L_w measured at 10 K for these GaN/Al_xGa_{1-x}N MQWs is plotted in Fig. 5, which shows that highest QE are achieved when L_w is between 12 and 42 Å. The uncertainty in the integrated emission intensity is mainly due to the slight variations in crystal growth between different runs. However, the general trend shown here is

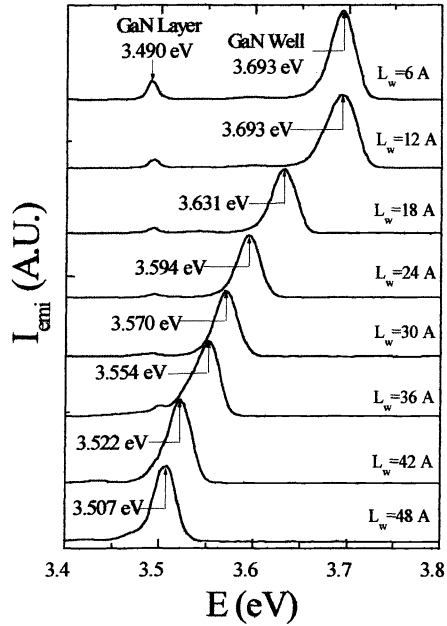


Fig. 2 The cw PL spectra measured at 10 K for the GaN/Al_xGa_{1-x}N MQW samples with well width varying from 6 to 48 Å and a fixed barrier thickness of 50 Å.

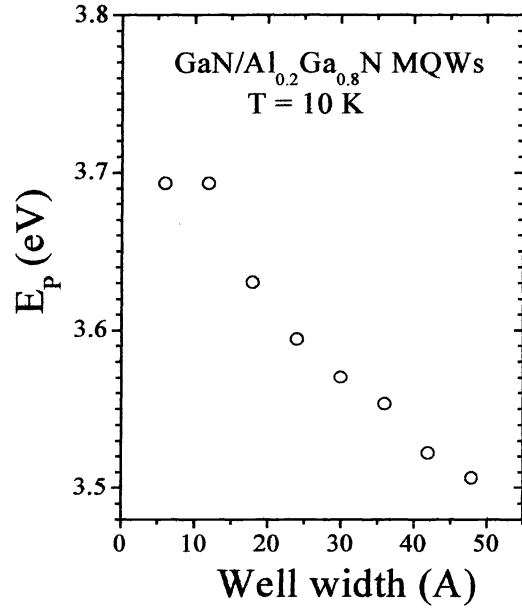


Fig. 3 FWHM of the well emission peak vs well width for the GaN/Al_xGa_{1-x}N MQW samples with well width varying from 6 to 48 Å and a fixed barrier thickness of 50 Å.

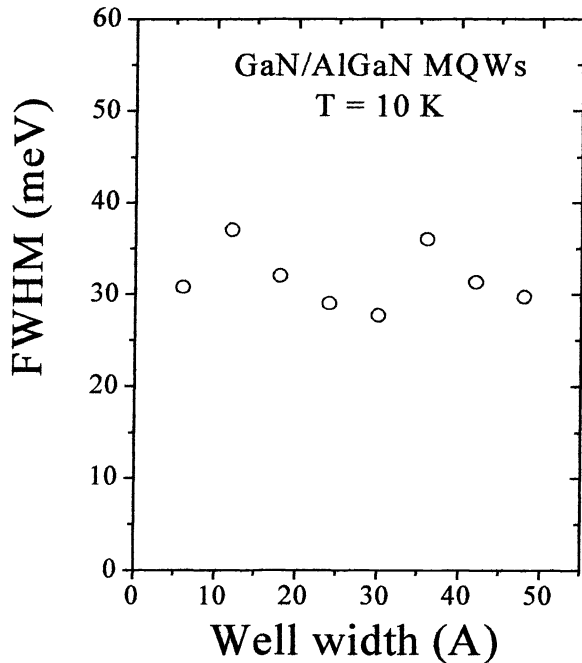


Fig. 4 FWHM of the well emission peak vs well width for the 50 Å barrier GaN/Al_xGa_{1-x}N MQWs.

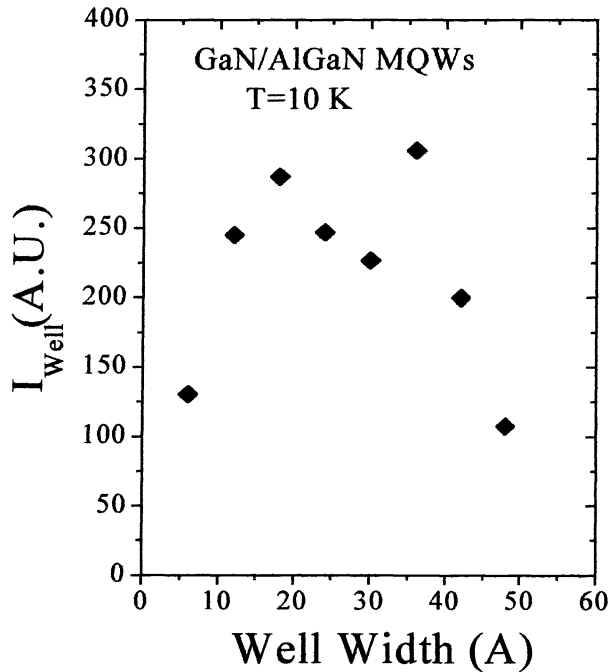


Fig. 5 Integrated emission intensity of the well emission peak vs well width for the 50 Å barrier GaN/Al_xGa_{1-x}N MQWs.

still quite clear despite the large experimental uncertainties. The high QE are resulted from an improved quantum well quality, a reduced nonradiative recombination rate, and a decreased piezoelectric effect in these MQWs.

The time-resolved spectra of the 48 Å GaN/Al_xGa_{1-x}N MQWs are presented in Fig. 6, where the well emission peak position demonstrates a total red shift with delay time of only about 5 meV. Similar behaviors have been observed for all GaN/Al_xGa_{1-x}N MQW samples studied here, implying the contribution from the piezoelectric field is negligibly small in GaN/Al_xGa_{1-x}N MQWs studied here. Previous studies have shown the time-resolved spectra of the well emission of GaN/Al_xGa_{1-x}N MQW samples ($L_w \geq 40$ Å) grown under different conditions to exhibit a large redshift (~ 60 meV) with delay time due to the presence of a strong piezoelectric effect together with the photoexcited carrier screening [7]. It is well known that the piezoelectric field will cause a spatial separation of the electron and hole wavefunctions and hence a large redshift of the well emission peak with respect to the GaN epilayers as well as a reduction of the radiative recombination rate (or QE)[3-7]. It seems that the piezoelectric field is greatly reduced and the QE are thus enhanced in these GaN/Al_xGa_{1-x}N MQWs grown under the optimal GaN-like growth conditions by MOCVD [8].

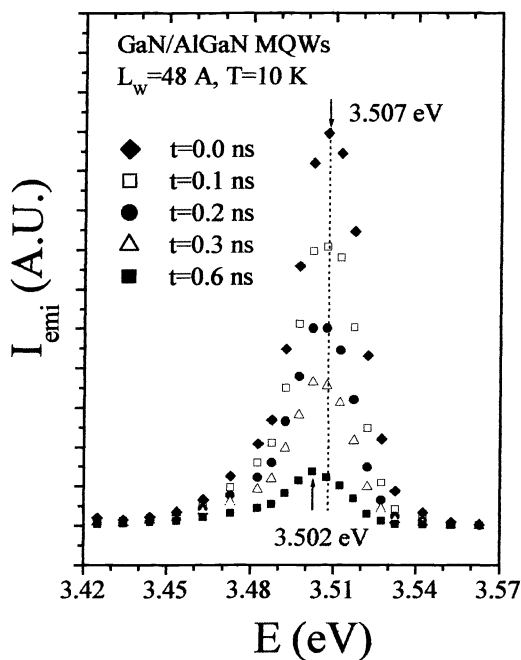


Fig. 6 Time-resolved PL spectra of the 48 Å well (and 50 Å barrier) GaN/Al_xGa_{1-x}N MQWs show a total red-shift with delay time of about 5 meV.

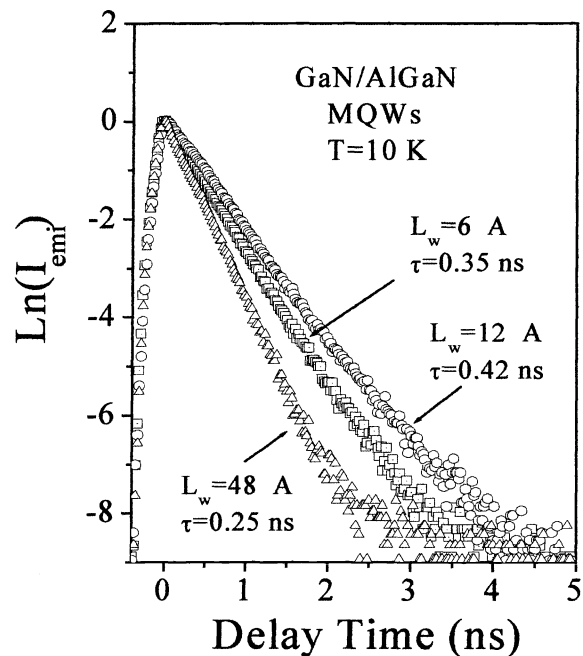


Fig. 7 PL decay profiles measured at 10 K from the well transitions of the 50 Å barrier GaN/Al_xGa_{1-x}N MQWs with $L_w = 6, 12,$ and 48 Å, respectively.

In addition to the reduced piezoelectric effect, the high QE achieved in the GaN/Al_xGa_{1-x}N MQWs with L_w between 12 and 42 Å can be attributed to the reduced nonradiative recombination rate as well as the improved quantum well interface quality. The decreased QE seen in GaN/Al_xGa_{1-x}N MQWs with larger L_w (>42 Å) suggests that the nonradiative recombination channels start to play an important role. This is consistent with the observation that the recombination lifetime of the well transition is shortest in the 48 Å GaN/Al_xGa_{1-x}N MQW sample. In Fig. 7, the PL temporal responses of the well transitions for three representative MQW samples are shown. We see that the recombination lifetime of the well transition in the 48 Å GaN/Al_xGa_{1-x}N MQWs is 0.25 ns, which is shorter than the value in the 6 Å (0.35 ns) or in the 12 Å (0.42 ns) GaN/Al_xGa_{1-x}N MQW sample. The low temperature lifetimes in all other GaN/Al_xGa_{1-x}N MQWs range in between 0.30 and 0.40 ns (not shown). The reduced recombination lifetime in the 48 Å well width GaN/Al_xGa_{1-x}N MQW sample is due to an increased nonradiative recombination rate. It is expected that the misfit dislocation density in the GaN-well regions increases sharply as the well width approaches the critical thickness of MQWs, which results in an enhanced nonradiative interface recombination rate and thus lower QE.

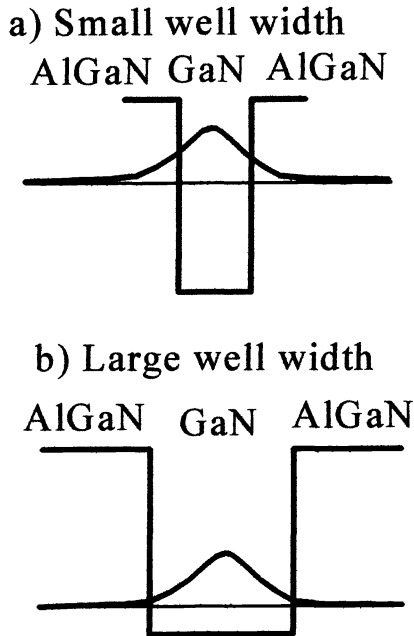


Fig. 8 The carrier leakage is enhanced in GaN/Al_xGa_{1-x}N MQWs with smaller well width than in those with larger well width.

On the other hand, the decreased QE in GaN/Al_xGa_{1-x}N MQWs with small L_w (less than 12 Å) is due to the enhanced carrier leakage to the underlying GaN epilayer. For MQWs with narrow L_w , the electron and hole wave functions will extend further into the barrier regions as illustrated schematically in Fig. 8, which leads to an increased (decreased) carrier recombination outside (inside) the well regions. As shown in Fig. 2, PL emission intensity at 3.490 eV from the underlying GaN epilayer is largest in the 6 Å well GaN/Al_xGa_{1-x}N MQW sample and decreases as L_w increases. This clearly indicates that the carrier leakage from the well regions to the underlying GaN epilayer increases with a decrease of L_w .

The temperature variations of the recombination lifetime and emission intensity have been measured for these MQW samples. For GaN/Al_xGa_{1-x}N MQW samples with $L_w < 48$ Å, the lifetime increases linearly with temperature up to 80 K, which implies that the radiative exciton recombination dominates in these MQWs at low temperatures. For $L_w = 48$ Å, a linear increase of lifetime with temperature is not observed due to an increased nonradiative recombination rate. The overall trend of the well width dependence of the integrated emission intensity is similar to that shown in Fig. 5 for all temperatures.

2.2 Barrier width dependence

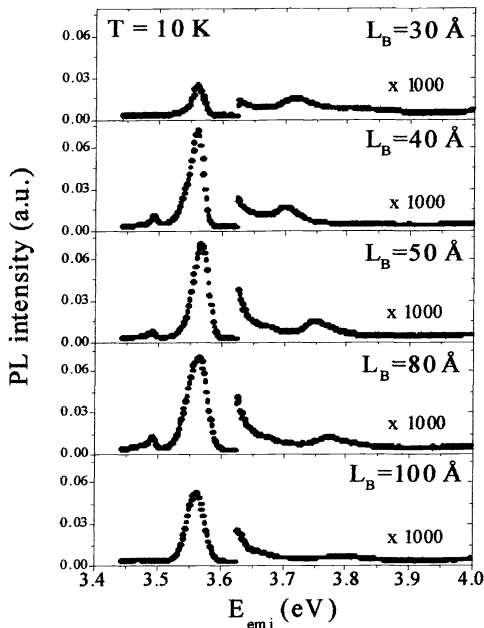


Fig. 9 CW PL spectra of a set of 30 Å well GaN/Al_xGa_{1-x}N MQW samples with varying barrier widths, $L_B = 30, 40, 50, 80,$ and 100 Å, measured at 10 K. The MQW structures are grown under identical conditions.

The low temperature ($T = 10$ K) PL spectra of the 30 Å well GaN/Al_xGa_{1-x}N MQW samples with various barrier widths of $L_B = 30, 40, 50, 80,$ and 100 Å are presented in Fig. 9. The position of the dominant emission peak at ~ 3.56 eV (10 K) in these spectra is almost independent of the barrier width and is due to the excitonic transition from the GaN wells. The full width at half maximum (FWHM) of the transition line from the wells is around 20 - 30 meV, which is again among the better values reported for the GaN/AlGa_{1-x}N MQW system [2-10]. The PL spectra also show a transition line with a lower emission intensity around 3.49 eV, which results from the underneath GaN epilayer.

One of the features exhibited by these 30 Å well MQW structures is that the excitonic transition peak resulting from the well regions is significantly blue shifted with respect to the GaN epilayers by about 70 meV (10 K). The observed spectral blueshift here suggests that the quantum confinement dominates the well known piezoelectric and polarization effects in these MOCVD grown MQW structures. The time-resolved PL spectral peak positions of the well transitions in these samples shift toward lower emission energies by less than 10 meV as the delay time increases from 0 to 0.8 ns, similar to that shown in Fig. 6. The magnitude of the redshift decreases with a decrease of L_B .

Another important feature shown by these 30 Å well MQW structures is that they exhibit a ratio of well emission intensity to barrier emission intensity of about 10^4 at 10 K. Moreover, the barrier emission intensity further decreases as temperature increases and drops to a signal level which is below the sensitivities of our detection systems when the temperature is above 200 K. This is

highly preferred for laser and LED applications, since one important issue in the laser and LED structural design is to maximize the optical emission or quantum efficiency in the quantum confined states in the well regions, while any optical transitions from the barrier regions represent a loss to optical gain.

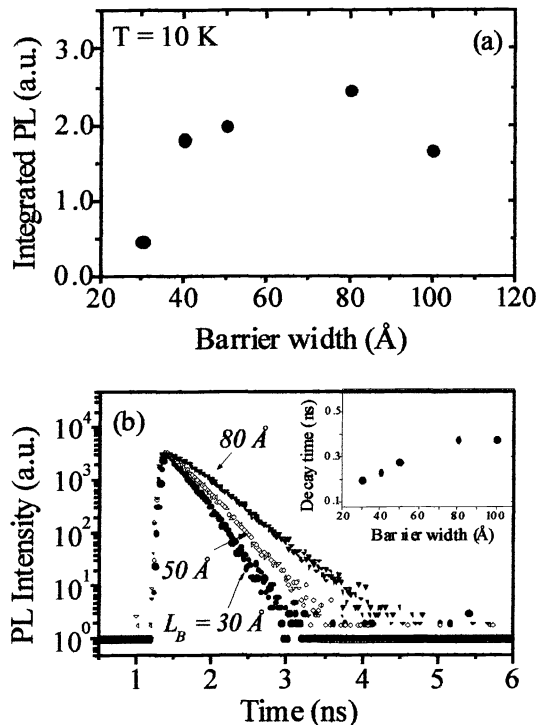


Fig. 10 (a) Integrated PL intensity of the well transition for the GaN/Al_xGa_{1-x}N MQW samples as a function of L_B measured at 10 K. (b) The temporal responses of the well transitions in the GaN/Al_xGa_{1-x}N MQW samples for various barrier widths at 10 K. The inset shows the barrier width dependence of the decay lifetime for the well transition.

The barrier width dependence of the integrated PL intensity of the well transition for these 30 Å well MQW structures can also be obtained from Fig. 9, which is plotted in Fig. 10(a). The total integrated PL intensities of these MQW samples are reduced only by one order of magnitude as the temperature rises from 10 to 300 K (not shown), indicating high PL efficiencies even at room temperature. The most important result shown in Fig. 10(a) is that the integrated PL intensities (or QE) of these MQW samples increase monotonously with an increase of the barrier width up to 80 Å.

The decay lifetime for the well transitions increases almost linearly from 0.2 ns to 0.4 ns when the barrier width varies from 30 to 80 Å. This is clearly illustrated in Fig. 10(b), where the PL temporal responses as well as the barrier width dependence of the PL decay lifetime are shown for the well transitions. Furthermore, a linear increase of the well transition lifetime with temperature has been observed in these MQW structures when the barrier widths is below 100 Å (not shown), which reflects that the radiative exciton recombination dominates in these MQW samples. The enhanced decay lifetime with the barrier width up to 80 Å shown in Fig. 10(b) is consistent with the QE enhancement with the barrier width shown in Fig. 10(a). For the 100 Å barrier MQW sample studied here, the well transition lifetime decreases with temperature (not shown), which is an indication of increased nonradiative recombination rates at higher temperatures in this MQW sample.

Our experimental results of the barrier width dependence of the PL efficiency and decay lifetime can be understood in terms of the barrier width dependent nonradiative interface recombination rate in MQWs, R_{nr} , which can be described by

$$R_{nr} \propto \left| \psi_{interface}^{SL} \right|^2 \cdot N_{interface}^{DL} \quad (1)$$

where $\psi_{interface}^{SL}$ and $N_{interface}^{DL}$ denote the electron (and hole) wavefunctions and the density of misfit dislocations at the interface, respectively. Thus two distinct mechanisms predominantly control the recombination rates and hence the quantum efficiencies in MQWs. For $L_B \lesssim 80$ Å, $N_{interface}^{DL}$ does not show a strong barrier dependence. Thus for the MQW samples with $L_B \lesssim 80$ Å, the reductions of the QE and decay lifetime with a decreased barrier width are mainly caused by an increased nonradiative recombination rate due to the enhanced probabilities of the electron and hole wavefunctions at the interfaces as well as in the AlGa_xN barriers. This situation is schematically illustrated in Fig. 11(a), where the electron wavefunction distributions for two representative L_B are shown, which indicates that $\psi_{interface}^{SL}$ decreases with an increase of L_B . Previously, reductions in the well emission intensities in MQWs of narrower barrier widths have been observed for the GaAs/AlGaAs MQW system [12].

On the other hand, the decrease of the QE and the lifetime behavior in the 100 Å barrier MQW can be accounted for by the concept of critical thickness. The critical thickness h_c of Al_xGa_{1-x}N epilayers on GaN as a function of Al molar fraction x has been calculated to be around 100 Å for $x \sim 0.2$ [13-15]. When L_B is approaching the critical thickness value h_c , strain is relieved

by the creation of misfit dislocations at the interfaces, a situation is being schematically illustrated in Fig. 11(b). Our results seem to further corroborate the fact that the critical thickness of the $\text{Al}_x\text{Ga}_{1-x}\text{N}/\text{GaN}$ ($x \sim 0.2$) MQW system is around 100 Å.

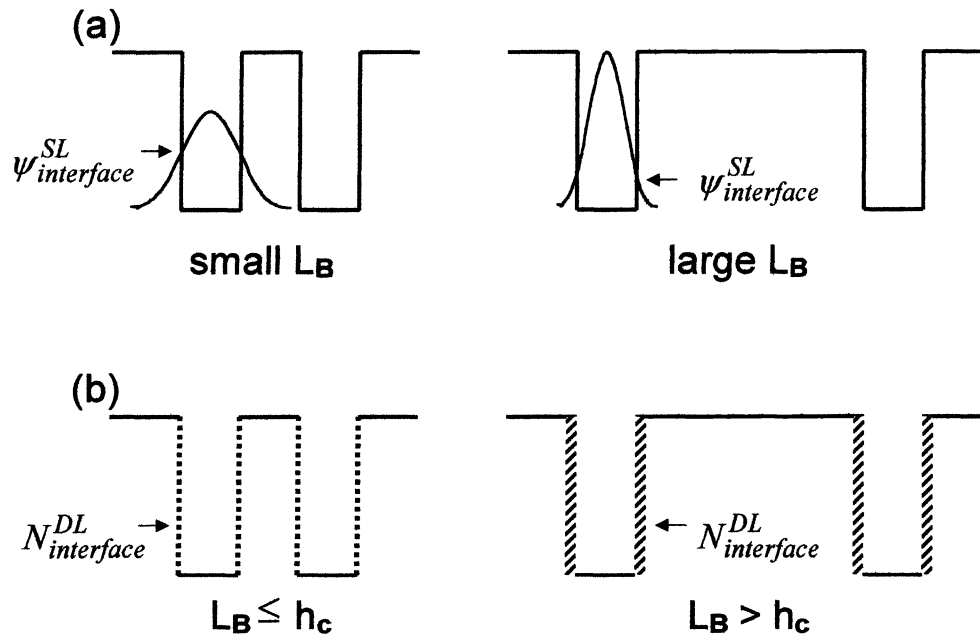


Fig. 11(a) Schematic diagrams showing the electron wavefunction distributions in MQWs for two representative barrier widths. The probability of the electron wavefunction at the interfaces as well as in the barriers decreases with an increase of the barrier width; (b) schematic diagram showing the misfit dislocation density at the interfaces in the $\text{GaN}/\text{Al}_x\text{Ga}_{1-x}\text{N}$ MQWs. The widths of the dotted lines represent the density of the misfit dislocations which increases sharply as L_B approaches h_c , where L_B and h_c denote the barrier width and the critical thickness, respectively.

2. SUMMARY

$\text{GaN}/\text{Al}_x\text{Ga}_{1-x}\text{N}$ and $\text{In}_x\text{Ga}_{1-x}\text{N}/\text{GaN}$ MQWs with varying structural parameters have been grown by our MOCVD system under the GaN-like conditions. We have shown that the optimal GaN/AlGaN ($x \sim 0.2$) MQW structures are those with well widths ranging from 12 and 42 Å and barrier widths ranging from 40 to 80 Å. When well width L_w is below 12 Å, the carrier leakage to the underlying GaN epilayers and the nonradiative interface recombination become prominent, while in MQWs with well width $L_w > 42$ Å the nonradiative recombination rate is increased due to L_w approaching the critical thickness of MQWs. For the barrier width dependence, when the barrier width is below the critical thickness, the nonradiative recombination rate increases with a decrease of the barrier width due to the enhanced probabilities of the electron and hole wavefunctions at the interfaces as well as in the AlGaN barriers. On the other hand, the misfit dislocation density increases as the barrier width approaches the critical thickness, which can result in an enhanced nonradiative interface recombination rate. An important feature shown by these MQW structures grown under the GaN-like conditions is that they exhibit a ratio of well emission intensity to barrier emission intensity of about 10^4 at 10 K. This is highly preferred for laser and LED applications, since one important issue in the laser and LED structural design is to maximize the optical emission or quantum efficiency in the quantum confined states in the well regions, while any optical transitions from the barrier regions represent a loss to optical gain.

ACKNOWLEDGEMENTS

The research is supported by DOE (96ER45604/A000), NSF (DMR-9902431 and INT-9729582), ARO, BMDO, and ONR.

REFERENCES

a) E-mail : jiang@phys.ksu.edu

- [1] H. Morkoç, S. Strite, G. B. Gao, M.E. Lin, B. Sverdlov, and M. Burns, *J. Appl. Phys.* **76**, 1363 (1994).
- [2]. M. Smith, J. Y. Lin, H. X. Jiang, A. Salvador, A. Botchkarev, W. Kim, and H. Morkoç, *Appl. Phys. Lett.* **69**, 2453 (1996).
- [3]. M. Leroux, N. Grandjean, J. Massies, B. Gil, P. Lefebvre, and P. Bigenwald, *Phys. Rev. B* **60**, 1496 (1998).
- [4]. J. S. Im, H. Kollmer, J. Off, A. Sohmer, F. Scholz, and A. Hangleiter, *Phys. Rev. B* **57**, R9435 (1998).
- [5]. P. Lefebvre, J. Allegre, B. Gil, H. Mathieu, N. Grandjean, M. Leroux, J. Massies, and P. Bigenwald, *Phys. Rev. B* **59**, 15363 (1999).
- [6]. H. Morkoc R. Cingolani, W. Lambrecht, B. Gil, H. X. Jiang, J. Y. Lin, D. Pavlidis, and K. Shenai, *MRS Internet J. Nitride Semiond. Res.* **4S1**, G1.2 (1999).
- [7]. H. S. Kim, J. Y. Lin, H. X. Jiang, W.W. Chow, A. Botchkarev, and H. Morkoç, *Appl. Phys. Lett.* **73**, 3426 (1998).
- [8] K. C. Zeng, J. Li, J. Y. Lin, and H. X. Jiang, *Appl. Phys. Lett.* **76**, 864 (2000).
- [9] K. C. Zeng, J. Li, J. Y. Lin, and H. X. Jiang, *Appl. Phys. Lett.* **76**, 3040 (2000).
- [10] Enu-joo Shin, J. Li, J. Y. Lin, and H. X. Jiang, *Appl. Phys. Lett.* **77**, 1170 (2000).
- [11] <http://www.phys.ksu.edu/area/GaNgroup/>
- [12]. M. Krahl, D. Bimberg, R. K. Bauer, D. E. Mars, and J. N. Miller, *J. Appl. Phys.* **67**, 434 (1990).
- [13]. J. Qu, J. Li, and G. Zhang, *Solid State Commun.* **107**, 467 (1998).
- [14]. W. G. Perry, M. B. Bremser, T. Zheleva, K. J. Linthicum, and R. F. Davis, *Thin Solid Films* **324**, 107 (1998).
- [15]. S. Krishnankutty, R. M. Kolbas, M. A. Khan, J. N. Kuznia, J. M. Van Hove, and D. T. Olson, *J. Electronic Materials*, **21**, 437 (1992).